

5. Yu. P. Zheltov, Mechanics of Oil and Gas Bearing Beds [in Russian], Nedra, Moscow (1975).
6. Yu. A. Buevich, "Structural and mechanical properties and filtering in elastic fissured porous material," *Inzh.-Fiz. Zh.*, 46, No. 4, 593-600 (1984).
7. M. G. Alishaev, "Numerical calculations of the elastic regime for the case of transition from constant yield to fixed bottom-hole pressure," in: *Present-Day Problems and Mathematical Methods of the Theory of Filtration/Abstracts of Papers*, Moscow (1984), pp. 31-32.
8. Yu. A. Buevich and V. S. Nustrov, "Nonlinear filtering in fissured porous materials," *Inzh.-Fiz. Zh.*, 48, No. 6, 943-950 (1985).
9. D. V. Kutovaya, "The effect of external pressure on the filtering properties of fissured rocks and opening of the fissures," *Neftyanaya i Gazovaya Promyshlennost'*, No. 1 (1962).
10. É. A. Avakyan and A. T. Gorbunov, "Determination of the parameters of fissured beds," in: *Theory and Practice of Crude Production [in Russian]*, Nedra, Moscow (1971), pp. 223-226.
11. J. A. Barker and J. H. Black, "Slug tests in fissured aquifer," *Water Resour. Res.*, 19, No. 6, 1558-1564 (1983).
12. V. M. Dobrynin, *Deformations and Changes of the Physical Properties of Oil and Gas Reservoirs [in Russian]*, Nedra, Moscow (1970).
13. J. E. Gale, "Flow and transport in fractured rocks," *Geosci. Canada*, 9, No. 1, 79-81 (1981).
14. A. Kh. Shakhverdiev, "Investigation of the filtering of a homogeneous liquid in deformed purely fissured reservoirs," *Izv. Akad. Nauk AzSSR, Ser. Nauk Zemle*, No. 1, 80-85 (1983).
15. E. S. Romm, *Filtering Properties of Fissured Rocks [in Russian]*, Nedra, Moscow (1966).
16. T. N. Krechetova and E. S. Romm, "Correlation of the principal components of the stress and permeability tensors of porous media," *Izv. Akad. Nauk SSSR, Mekh. Zhidk. Gaza*, No. 1, 173-177 (1984).
17. M. I. Shvidler, "Filtering transfer in media with random structure," in: *Fifth All-Union Congress on Theoretical and Applied Mechanics, Synopses of Papers*, Alma-Ata (1981), pp. 358-359.
18. R. D. Evans, "A proposed model for multiphase flow through naturally fractured reservoirs," *Soc. Petrol. Eng. J.*, 22, No. 5, 669-680 (1982).
19. I. N. Sneddon, *Fourier Series*, Routledge & Kegan (1973).
20. M. Masket, *Flow of Homogeneous Liquids in a Porous Medium [Russian translation]*, Gostoptekhizdat, Moscow-Leningrad (1949).

ISOTHERMAL FLUID FLOW IN A PACKING OF SPHERES

V. I. Volkov

UDC 532.436

Simultaneous measurements of the velocity profiles inside and behind a packing made of spheres are used to establish the pattern of isothermal flow of a fluid inside the packing.

Several investigations have found that the velocity field after a granular bed may be quite different from the velocity field inside the bed [1, 2]. We therefore made use of studies which determined the fluid velocity inside the bed. Analysis of these works showed that all of the contact methods of measurement give a planar or nearly planar velocity profile if the size of the transducer is comparable to or greater than the size of a granule of the porous medium [2-4].

It has been established by all of the noncontact and diffusive methods of determining velocity that the fluid velocity is significantly higher near the wall than in the center of the packing [5-7]. This discrepancy in the findings is evidently due to the fact that in the measurement of velocity from the heat and mass transfer from a transducer comparable in size to the granule size in the bed, one is actually determining the hydrodynamic situation

Altai State University, Barnaul. Translated from *Inzhenerno-Fizicheskii Zhurnal*, Vol. 49, No. 5, pp. 827-833, November, 1985. Original article submitted September 11, 1984.

around this transducer without allowance for the direction of velocity. Measurement by time-of-flight methods involves finding the longitudinal component of velocity averaged over the free area between granules in one section of the packing. If the free area is unevenly distributed over the cross section, then fluid flow rate will be greater at those sites in the packing where there are more free passages for the flow. This reasoning, which at first seems obvious, is contradicted by the results obtained in [8]. Here, some of the spheres were attached to the walls of the test section to create uniform porosity over the cross section. Nevertheless, the local velocity of the fluid at the wall in this study was 10% greater than in the center of the packing in an appreciably turbulent flow regime ($Re \geq 4800$; henceforth, the Reynolds number is figured from the flow-rate velocity in an empty test section and the diameter of the spheres). Moreover, it is still uncertain by how much the velocity at the wall of a random packing exceeds the velocity in the center and how this relative increase depends on the Reynolds number. All of the authors have obtained different relative increases in velocity at the wall. For example, whereas Aerov and Umnik found a 30% relative increase, Abaev, Popov, Smirnov, and other investigators found a sixfold increase in fluid velocity at the wall relative to the velocity in the center of the packing [6, 7].

The above-mentioned noncontact and contact methods do not have sufficient resolving power and do not make it possible to establish the velocity profile in an individual pore of a granular bed. More local and exact methods such as thermoanemometric or laser-Doppler methods have thus far been used only to measure flow velocity in regular packings. For example, we know of two studies which used hot-wire anemometers to obtain velocity profiles in individual cells of cubic and rhombic packings [8, 9] and one study [10] which used a laser-Doppler anemometer (LDS) to measure fluid velocity at individual points of a tetrahedral packing with a Reynolds number of 0.04. The limited amount of data on the velocity fields in these measurements makes it impossible to ascertain the structure and features of motion of the flow not only inside a random packing of spheres, but also inside simple models of a porous medium such as a cubic packing of spheres. Following [11], we will represent a random packing as a mixture of cubic and tetrahedral packings. We then examine the mean-velocity profiles separately for the tetrahedral and cubic packings. Assuming that the geometry of the packing has a decisive effect on the hydrodynamics, we find the limits of nonuniformity of the mean-velocity profile in the random packing. The tetrahedral packing of spheres has the greatest drag and the lowest porosity. Also, the path of the fluid particles is most sinuous in this packing. In the cubic packing of spheres, sinuousness and drag are minimal and porosity is maximal. Regardless of the form of the packing inside the test section, mainly a cubic packing is formed near the wall [6].

Thus, fluid velocity at the wall of a tetrahedral packing exceeds the velocity in the center by as large a factor as is possible. Fluid velocity in the center of a cubic packing, meanwhile, exceeds the velocity at the wall by as large a factor as is possible compared to any other types of packings - including a random packing.

We obtain the profile of mean velocity in the tetrahedral packing by averaging five local velocity profiles presented in [10] (Fig. 1).

We similarly obtain the mean-velocity profile in a cubic packing of spheres by averaging local velocity profiles reported in [12] in four cross sections separated by a distance equal to half the radius of one sphere and on nine measurement lines in each section (Figs. 2 and 3). Sections A and C were located in the tenth and eleventh layers of spheres from the beginning of the packing, respectively. Sections B and D correspond to the widest and narrowest sections of the cubic packing. Velocity was determined in 1.5-mm intervals along each measurement line. Nine spheres in all were located in each cross section of the test section.

To compare the mean velocity with the flow-rate velocity, velocity was measured on thirteen measurement lines in each of the four sections A, B, C, and D in Fig. 2. These lines are denoted by primes in section D of Fig. 2. The measured velocity field was used to determine the mean velocity, which differed no more than 5% from the flow-rate velocity. The LDA method was used to measure the Poiseuille velocity profile in cylindrical and planar channels [12] with a similar error. To exclude the corner effects of the rectangular test section with a cubic packing, in constructing the mean-velocity profiles in Figs. 2 and 3 we considered only the nine measurement lines located a distance from the wall greater than the radius of a sphere.

It is apparent from Fig. 1 that the mean velocity of the fluid at the wall of a tetrahedral packing is no more than twice as great as the flow-rate velocity and the velocity at

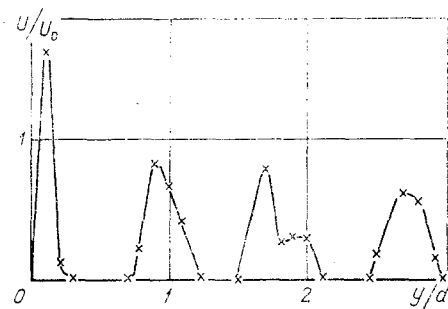


Fig. 1

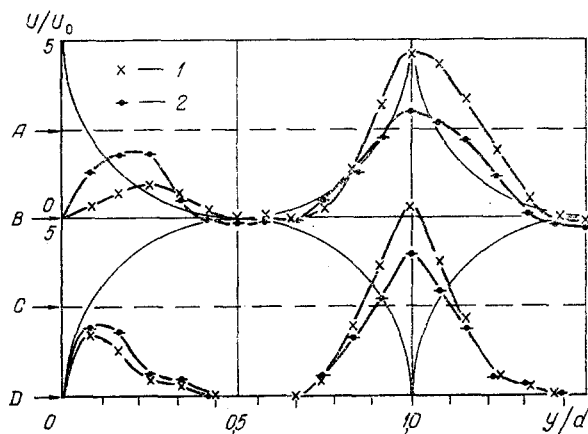


Fig. 2

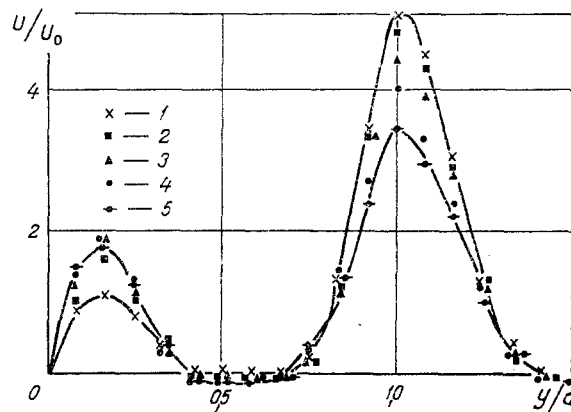


Fig. 3

Fig. 1. Profile of mean velocity U , referred to the flow-rate velocity U_0 , in an octahedral packing [10] with $2R/d = 6$. The reckoning was made from the wall of the test section.

Fig. 2. Profiles of mean relative velocities in sections B and D, respectively, in relation to the transverse coordinate, referred to the diameter of the spheres, with $2R/d = 3$: 1) $Re = 22$; 2) $Re = 500$.

Fig. 3. Profile of mean relative velocity in a cubic packing obtained by averaging the velocity fields in sections A, B, C, and D of Fig. 2: 1) $Re = 22$; 2) 60; 3) 110; 4) 260; 5) 500.

the center of the packing. Thus, in the case of low Reynolds numbers, the mean velocity at the wall of a random packing is no more than twice as great as the flow-rate velocity.

Figures 2 and 3 illustrate the opposite pattern, i.e., the mean velocity of the fluid at the center of the cubic packing may be five times greater than the velocity at the wall for low Reynolds numbers. However, with an increase in the Reynolds number to 500, the mean-velocity profile becomes more uniform across the test section, i.e., the mean velocities at the wall and the center of the cubic packing become equal. Although Figs. 2 and 3 show profiles of mean velocity for Reynolds numbers no greater than 500, measurements of velocity were made with an LDA at individual points of a cubic packing up to $Re = 2000$. Here, the maximum velocities at the wall and at the center of the test section with a cubic packing approached a common limit equal to the flow-rate velocity. Thus, it may be proposed that there are limits to the nonuniformity of the profile of mean velocity in a random packing. Thus, the mean fluid velocity at the center of such a packing - even with random formation of the cubic packing - may be no more than five times as great as the flow-rate velocity, while the mean velocity at the wall of a random packing may be no more than twice as great as the flow-rate velocity.

Let us check the above conclusions on a well-known profile of mean velocity inside a random packing obtained with an LDA on a test section of a diameter 7.5 times greater than the sphere diameter [12]. To measure the fluid velocity with an LDA in packings of spheres, the refractive indices of the fluid and spheres are chosen to be the same. View B in Fig. 4

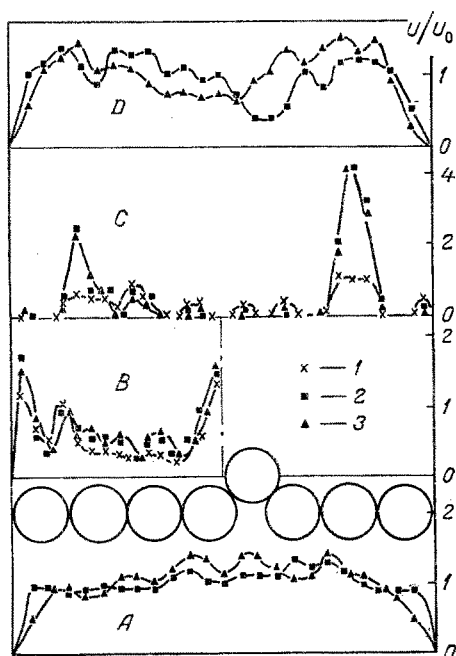


Fig. 4. Velocity profiles in a random packing with $2R/d = 7.5$: 1) $Re = 13$; 2) 54; 3) 100.

shows the mean-velocity profile in a random packing obtained with an LDA. This profile was obtained from 32 local velocity profiles with 10 repackings. At least three profiles were recorded in each repacking beginning at a distance from the beginning of the random packing greater than or equal to 14 sphere diameters. Here, the total length of the packing was equal to 25 sphere diameters. Figure 4 also shows velocity profiles at the inlet of the packing and at its outlet at a distance equal to 9 sphere diameters - sections A and D, respectively. One of the local velocity profiles inside the random packing, at a distance equal to 14.5 sphere diameters from the beginning of the packing, is shown in Fig. 4, view C. It is apparent from the figure that in the range of $Re = 13-100$, the mean velocity of the fluid in the wall region is no more than twice as great as the flow-rate velocity, and the mean fluid velocity at the center of the packing is also no more than twice as great as the latter. Thus, the assumption made regarding the character of fluid flow in a random packing on the basis of measurements in cubic and tetrahedral packings was not unfounded and can be used later to predict limiting flow regimes in actual packings.

Let us attempt to explain the difference in fluid flow in different packings.

Of the regular packings, the least and greatest sinuousness corresponds to the cubic and tetrahedral packings, respectively. "Wandering" of gas in a random packed bed and sinuousness at low Reynolds numbers were discussed earlier in [13], which did not explain how the increased sinuousness of the flow affects the mean-velocity profile. Measurements of fluid velocity in a random packing with an LDA make it possible to conclude that at Reynolds number of 10 or less, the fluid is nearly still in most of the cross section of the packing [12]. Only a few through channels are formed in a random packing (Fig. 4). Moving from layer to layer, a fluid particle can change location so much in the case of low Reynolds numbers that it moves nearly perpendicular to the vector of the external pressure gradient in most of the test section. Large-scale regions of stagnant zones are formed. Thus, it is hardly useful to deal with the fluid velocity profile inside a random packing averaged over the cross section of the packing in the case of low Reynolds numbers.

Sinuousness decreases with an increase in the Reynolds number, and the inertia of the fluid particles increases. They can now jump from layer to layer in the packing with a smaller change in the direction of the velocity vector. When the number $Re^* \sim 200$ is reached in an individual channel of the packing, there is a transition to turbulent flow in the mixing layer between the flow in this channel and the stagnant zone of fluid surround it [14].

Here, the Reynolds number Re^* was figured from the maximum velocity in the individual channel and the equivalent diameter of this channel. For example, in Figs. 3 and 4, the maximum values of relative velocity near the wall are reached at $Re \sim 100$. With a further increase in the Reynolds number, turbulent broadening of the velocity profile begins. Thus, the transition to turbulent flow begins earlier in the broader channels of the packing. After this transition, momentum losses increase in these channels as a result of the turbulent pulsations. This in turn leads to equalization of the maximum velocities in the through

channels with broad and narrow sections at high Reynolds numbers. Consequently, regardless of the channel diameter, with fully developed turbulent flow the profile of fluid velocity in each pore will be completely full. Meanwhile, the maximum velocities in the individual channels will be roughly equal and close to the flow-rate velocity inside the packing, i.e., the velocity in an empty test section divided by the porosity. To all appearances, only for such regimes of fluid flow will it be possible to agree with the observation of Jubota to the effect that fluid flow rate near the wall and at the center will be determined only by the number of cavities and that mean velocity will be higher where there is a large number of cavities [4]. At what Reynolds numbers does fully turbulent flow begin in a random packing? The studies done thus far do not give an unequivocal answer to this question. It follows from the experiments of Mickley et al. on a rhombic packing [8] that fluid velocity at the wall is 10% higher than fluid velocity at the center even at Reynolds numbers of 4800. Thus, developed turbulent flow begins in a rhombic packing at $Re > 5000$. In connection with this, it is possible to try to explain the nonuniformity of the velocity profile obtained in [8] with a uniform porosity across the packing as being the result of greater damping of turbulent pulsations near the wall compared to the center. The wall limits transverse pulsations of velocity to a greater degree than does a dense packing, which contains channels perpendicular to the main flow. The greater the transverse turbulent pulsations, the more sinuous the path of the fluid particles. Thus, a strictly uniform velocity profile should be expected in packings having not only uniform porosity but also uniform sinuousness over their cross sections.

Consequently, in the viscous regime of flow in packings, the flow moves mainly along the channels with the largest cross section, and the hydrodynamics is determined by the diameter of the channel and its sinuousness.

The effect of sinuousness decreases in the inertial flow regime. The mean velocity profile evens out across the test section. The transition from one regime to another does not occur at the same time over the cross section of the test section. Turbulence begins earlier in the channels with the greatest sinuousness and largest diameter. In a fully developed turbulent regime of fluid flow, the mean velocity profile inside the packing is determined by the number of cavities over its cross section.

It is interesting to compare the results obtained with earlier measurements made behind packings, where all authors obtained an increase in mean velocity at the wall relative to the center. Studies of the mean-velocity profile after a packing by means of an LDA showed that at low Reynolds numbers $Re \sim 10$ a series of jets is formed after the packing. These jets are twisted into individual vortices at a distance equal to several sphere diameters, while a large-scale annular vortex is formed at a distance equal to several channel diameters. The velocity in the center of this vortex may be directed counter to the external pressure gradient. With an increase in the Reynolds number, the annular vortex is destroyed and the velocity in the center of the channel, changing sign, becomes positive. Whereas the vortices from individual channels in the packing may be twisted in any direction in the center of the test section, in the channels near the wall they are twisted only from the wall toward the center of the test section. Stratified flow with laminar viscosity is preserved near the wall [14]. These differences in the wall and central parts of the packing lead to a nonuniform velocity profile after the packing (Fig. 4). In other words, eddy viscosity behind the packing is higher in the center of the test section than near the wall. This phenomenon was observed in a study of the equalizing effect of grates [15].

It follows from Fig. 4 that the velocity profiles inside a random packing do not adequately correspond to the velocity profiles after the packing, as was noted in [1, 2].

NOTATION

$Re = U_0 d / \nu$, Reynolds number; U_0 , flow-rate velocity of the fluid in a test section not filled with packing; d , diameter of spheres of packing; in the experiments using an LDA, $d = 0.0183$ m; $Re^* = U^* d_e / \nu$, Reynolds number figured from the maximum velocity U^* in an individual channel and the equivalent diameter of this channel; $d_e = 4S / \ell$, equivalent diameter of the channel; S , cross section of the channel at the narrowest part of the cubic packing; ℓ , wetted perimeter of cross section S ; R , radius or half-width of the test section with packing; y , transverse coordinate, reckoned from the wall of the test section with packing; ν , kinematic viscosity of the fluid.

LITERATURE CITED

1. J. J. Lerous and G. Froment, "Velocity, temperature, and conversion profiles in fixed bed catalytic reactors," *Chem. Eng. Sci.*, 32, No. 8, 853-861 (1977).
2. V. A. Kirillov, V. A. Kuz'min, V. I. P'yanov, and V. M. Kanaev, "Velocity profile in a packed bed," *Dokl. Akad. Nauk SSSR*, 245, No. 1, 159-162 (1979).
3. T. Akehato and K. Sato, "New distribution in packed beds," *Kagaku Kogaku*, 22, No. 7, 430-436 (1958).
4. Hiroshi Kubota, Minoru Jkeda, and Vasuhico Nishimira, "Note on flow-profile in packed beds," *Kagaku Kogaku*, 4, No. 1, 58-61 (1966).
5. E. J. Cairns and J. M. Prausnitz, "Velocity profiles in fluidized beds," *Ind. Eng. Chem.*, 51, No. 12, 1441-1444 (1959).
6. M. E. Aerov, O. M. Todes, and D. A. Narinskii, *Equipment with Packed Beds* [in Russian], Khimiya, Leningrad (1979), pp. 77-81.
7. G. N. Abaev, E. K. Popov, et al., "Results of a study of the aerodynamics of a granular bed on stands and in commercial reactors for synthesizing monomers for synthetic rubber," in: *Aerodynamics in Industrial Processes* [in Russian], Nauka, Moscow (1981), pp. 79-91.
8. D. F. Van der Merwe and W. H. Gauvin, "Velocity and turbulence measurements of air flow through a packed bed," *AIChE J.*, 3, 519-528 (1971).
9. H. S. Mickley, K. A. Smith, and E. I. Korchak, "Fluid flow in packed beds," *Chem. Eng. Sci.*, 20, No. 3, 237-246 (1965).
10. W. Johnston, A. Dybbos, and R. Edwards, "Measurement of fluid velocity inside porous media with a laser anemometer," *Phys. Fluids*, 18, No. 7, 913-914 (1975).
11. M. A. Gol'dshtik, "Theory of concentrated disperse systems," in: *Materials of an International Conference on Transport Processes in Packed and Fluidized Beds* [in Russian], ITMO im. A. V. Lykova, Minsk (1977), pp. 49-84.
12. V. I. Volkov, "Investigation of hydrodynamics and transport processes in fluidized beds," Author's Abstract of Candidate's Dissertation, Engineering Sciences, ITF Sib. Otd. Akad. Nauk SSSR, Novosibirsk (1982).
13. F. F. Kolesanov, *Movement of Gas Through a Layer of Lump Materials* [in Russian], Metallurgiya, Moscow (1956), pp. 43-65.
14. V. I. Volkov, V. A. Mukhin, and V. E. Nakoryakov, "Study of the flow structure in a porous medium," *Zh. Prikl. Khim.*, 34, No. 4, 838-842 (1981).
15. I. E. Idel'chik, *Aerodynamics of Industrial Equipment* [in Russian] Énergiya, Moscow (1964).